

## Supporting Information

### Calix[4]arene with a stiff upper rim bridge: spontaneous macrocyclization, structure, and dynamic behaviour

Vladimir A. Azov,<sup>1</sup> Jonas Warneke,<sup>2,3</sup> Ziyan Warneke,<sup>2</sup> Matthias Zeller,<sup>4</sup> Linette Twigge<sup>1</sup>

[1] Department of Chemistry, University of the Free State, P.O. Box 339, 9300 Bloemfontein, South Africa.

[2] Wilhelm-Ostwald-Institut für Physikalische und Theoretische Chemie, Universität Leipzig, 04103 Leipzig, Germany

[3] Leibniz-Institut für Oberflächenmodifizierung e.V. (IOM), Permoserstrasse 15, 04318 Leipzig, Germany

[4] Department of Chemistry, Purdue University, West Lafayette, IN 47907, United States

\* Corresponding author, E-mail: [azovv@ufs.ac.za](mailto:azovv@ufs.ac.za)

#### Table of Contents

Crystallographic data of <b>3</b>	S2
ORTEP plot of <b>3</b>	S3
NMR spectra of <b>3</b>	S4
Description of VT-NMR experiments	S6
MS spectra of <b>3</b>	S9
MS fragmentation experiments	S11
Computational details	S13

**Table S1.** Crystallographic date for 3.

Crystal data	
Chemical formula	C <sub>42</sub> H <sub>50</sub> O <sub>5</sub> ·0.078(C <sub>2</sub> H <sub>6</sub> O)
M <sub>r</sub>	638.38
Crystal system, space group	Triclinic, P <sup>-1</sup>
Temperature (K)	100
a, b, c (Å)	13.6255 (13), 17.2297 (17), 17.4046 (17)
α, β, γ (°)	109.4387 (14), 91.6526 (15), 105.8046 (15)
V (Å <sup>3</sup> )	3675.1 (6)
Z	4
Radiation type	Mo K $\alpha$
μ (mm <sup>-1</sup> )	0.07
Crystal size (mm)	0.41 × 0.35 × 0.25
Data collection	
Diffractometer	Bruker AXS SMART APEX CCD diffractometer
Absorption correction	Multi-scan, Apex2 v2013.4-1 (Bruker, 2013)
T <sub>min</sub> , T <sub>max</sub>	0.660, 0.746
No. of measured, independent and observed [I > 2σ(I)] reflections	61777, 21639, 14943
R <sub>int</sub>	0.036
(sin q/l) <sub>max</sub> (Å <sup>-1</sup> )	0.715
Refinement	
R[F <sup>2</sup> > 2σ(F <sup>2</sup> )], wR(F <sup>2</sup> ), S	0.053, 0.146, 1.03
No. of reflections	21639
No. of parameters	1126
No. of restraints	839
H-atom treatment	H-atom parameters constrained
Δρ <sub>max</sub> , Δρ <sub>min</sub> (e Å <sup>-3</sup> )	0.45, -0.24

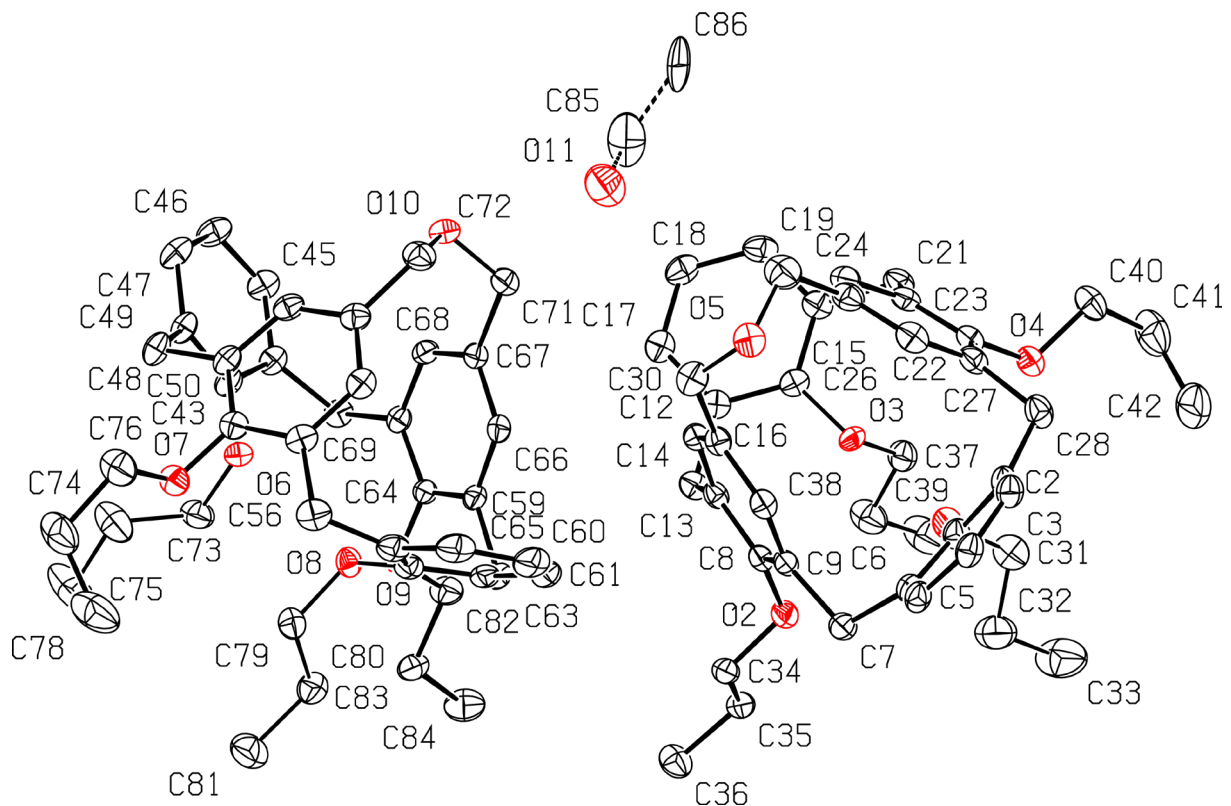


**Figure S1.** ORTEP plot of **3** showing two asymmetric calixarene molecules and disordered ethanol molecule. Only major orientations of the disordered fragments are shown. H-atoms are removed for clarity.

### Data processing

The data were reduced and corrected for absorption with the Bruker SAINT v7.66A software (Bruker, 2013). Structures were solved with SHELXS (Sheldrick, 2008) and refined with SHELXL 2019/2 (Sheldrick, 2015, 2019) and the ShelXle graphical interface (Hübschle *et al.*, 2011).

### Software

1. BRUKER AXS (2013). *Apex2 v2013.4-1*.
2. BRUKER AXS (2013). *SAINT V8.30C*.
3. Hübschle, C. B., Sheldrick, G. M. & Dittrich, B. (2011). *J. Appl. Crystallogr.* **44**, 1281–1284.
4. Sheldrick, G. M. (2008). *Acta Crystallogr. Sect. A Fundam. Crystallogr.* **64**, 112–122.
5. Sheldrick, G. M. (2015). *Acta Crystallogr. Sect. C - Struct. Chem.* **71**, 3–8.
6. Sheldrick, G. M. (2019). *SHELXL2019/2*.

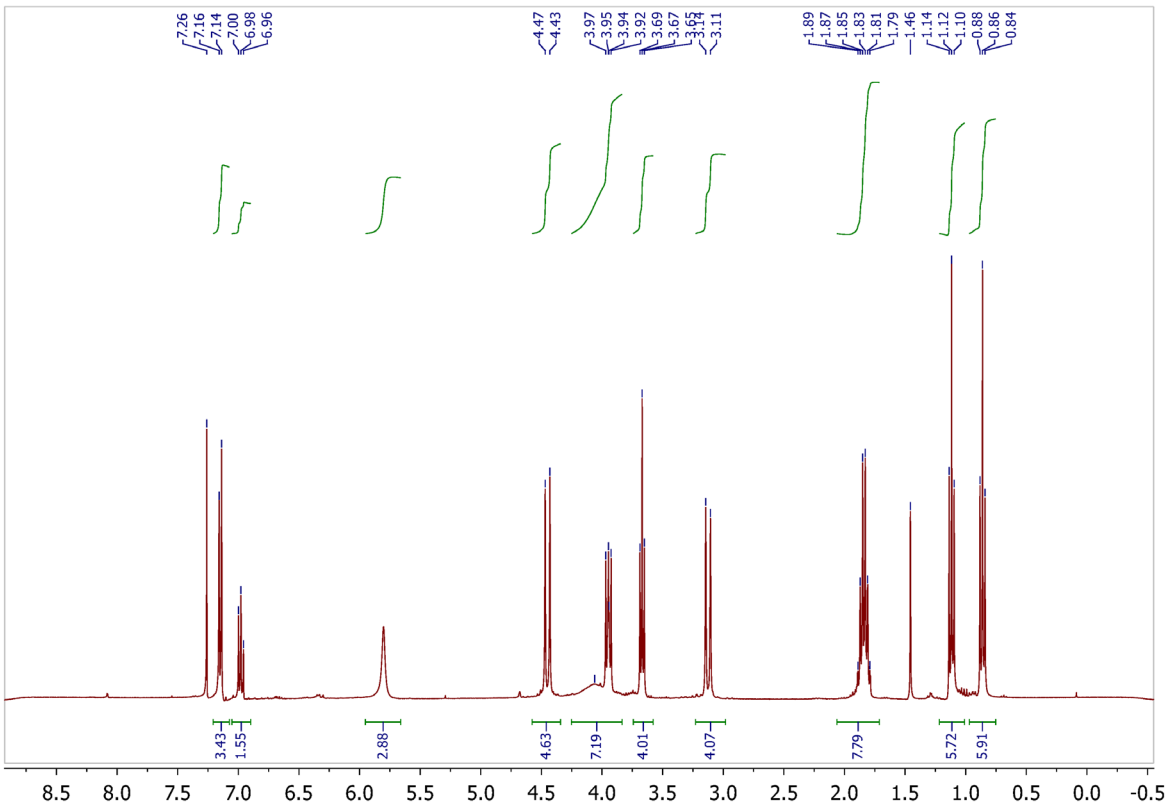


**Figure S2a.** <sup>1</sup>H NMR spectrum of compound 3 (600 MHz, CDCl<sub>3</sub>) measured at 328 K.

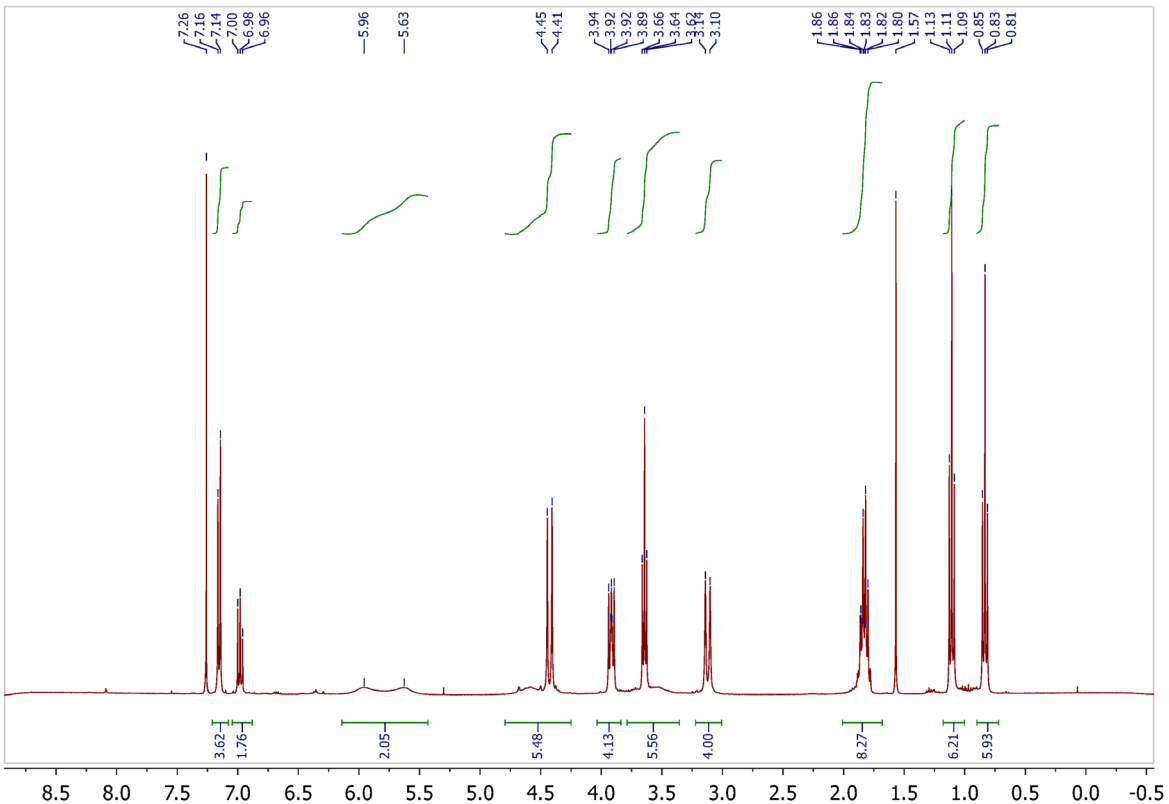


**Figure S2b.** <sup>1</sup>H NMR spectrum of compound 3 (600 MHz, CDCl<sub>3</sub>) measured at 293 K.

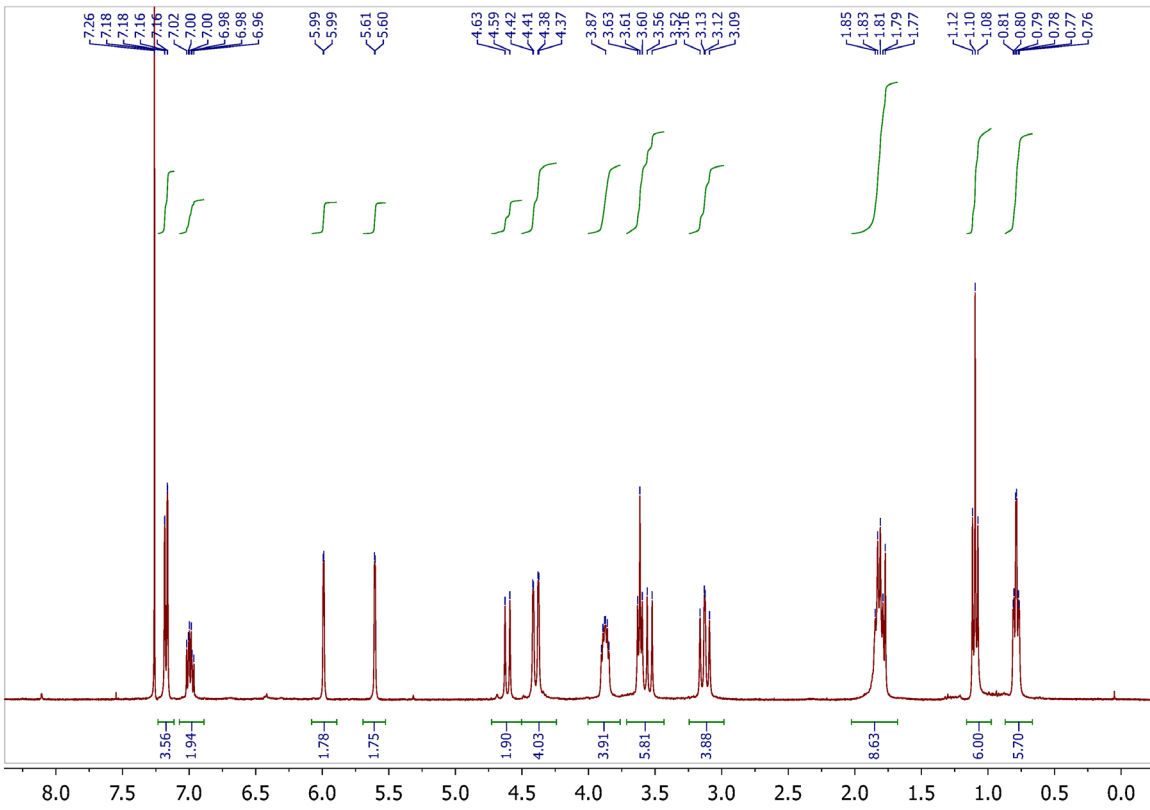


**Figure S2c.**  $^1\text{H}$  NMR spectrum of compound 3 (600 MHz,  $\text{CDCl}_3$ ) measured at 263 K.

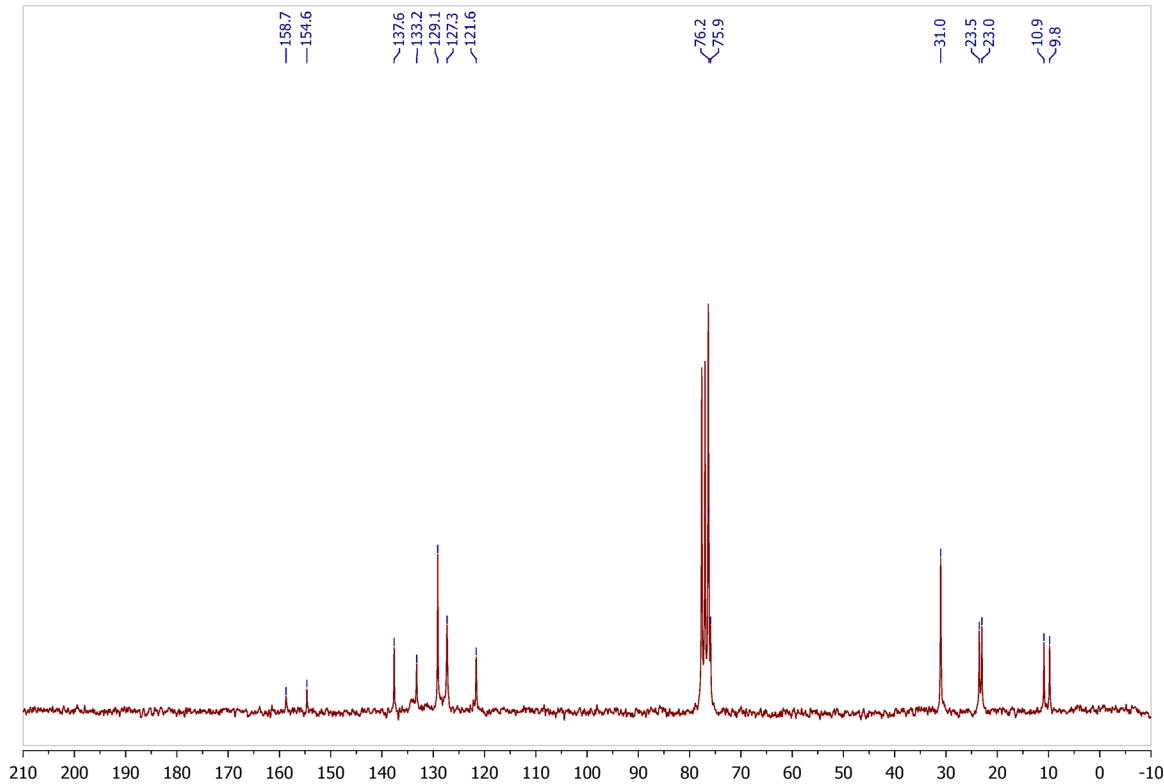


**Figure S3.**  $^{13}\text{C}$  NMR spectrum of compound 3 (50 MHz,  $\text{CDCl}_3$ ) measured at 293 K.

## VT-NMR experiments and fitting of $^1\text{H}$ NMR spectra.

A solution of compound **3** in  $\text{CDCl}_3$  was placed into a standard 5 mm NMR tube and loaded into a Bruker Avance DRX600 NMR spectrometer. The probe was cooled or heated to the desired temperature and allowed to equilibrate for ca. 10-15 min before the spectrum was recorded. Fourier transformations of FIDs were performed using the Bruker Topspin software.

The Topspin software was also used to perform line-shape analysis and for fitting of the NMR spectra. Fitting was performed for the signals of aromatic  $\text{H}^\text{H}$  protons, which did not overlap with any other NMR resonances, had mutual separation convenient for fitting, and coalesced close to room temperature. A chemical shift of  $\Delta\nu = 139 \text{ Hz}$  between two coalescing resonances was determined for two spectra measured at 213 and 233 K temperatures, which is far below the coalescence temperature. For each modelled spectrum measured at a given temperature, the line width and peak separation  $\Delta\nu$  were determined, and the spectral fitting was performed by changing the value of the exchange rate constant  $k_r$  to achieve the best fit. An Eyring plot was derived by plotting the data on a diagram with  $1/T$  on the  $x$ -axis vs.  $\ln(k_r/T)$  on the  $y$ -axis, according to the equation (1):

$$\ln\left(\frac{k_r}{T}\right) = -\frac{\Delta H^\ddagger}{RT} + \frac{\Delta S^\ddagger}{R} + \ln\left(\frac{k_b}{h}\right) \quad (1)$$

where  $\ln(k_b/h) = 23.760$ .

Thermodynamic parameters for the exchange between two degenerate conformations were derived using equations (2,3) and the *intercept* and *slope* derived from the Eyring plot:

$$\Delta H^\ddagger = -R \cdot \text{slope} \quad (2)$$

$$\Delta S^\ddagger = -R \cdot (\text{intercept} - \ln(k_b/h)) \quad (3)$$

Equation (4) was used to calculate the free energy of activation  $\Delta G^\ddagger$  at the temperature of coalescence of an equally populated two-site system:

$$\Delta G^\ddagger = aT \left[ 9.972 + \log\left(\frac{T_c}{\Delta\nu}\right) \right] \quad (4)$$

where  $T$  is the temperature in Kelvin,  $\Delta\nu$  [Hz] the chemical shift between two coalescing resonances in the absence of exchange, and  $a = 1.914 \times 10^{-2}$  for  $\Delta G^\ddagger$  units of kJ/mol.

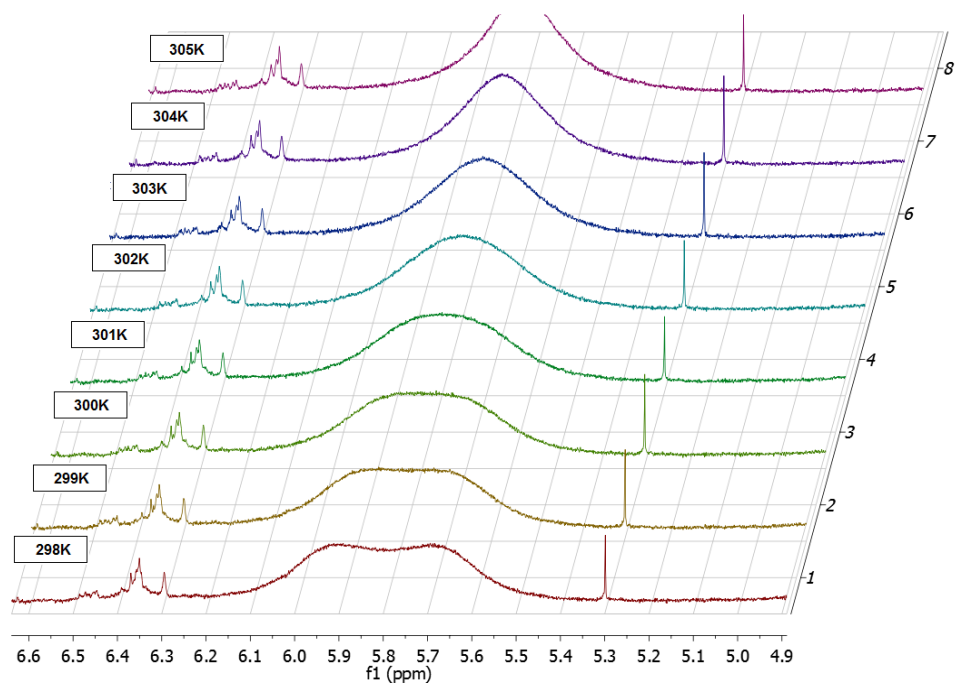


**Figure S4.**  $^1\text{H}$  VT-NMR scan of **3** in the 298–305 K range in  $\text{CDCl}_3$ , featuring the behavior of the resonances at 5.6–6 ppm range (*o*-hydrogens to the bridges) near the coalescence temperature.

**Table S2.** Rate constants  $k$  ( $\text{s}^{-1}$ ) and other parameters for the conformer exchange of **3** at different temperatures,  $T$  (K).

T (K)	k ( $\text{s}^{-1}$ )	k/T	1/T (K $^{-1}$ )	ln(k/T)
213	4,941E-03	2,32E-05	0,00469	-10,671
233	8,559E-02	0,000367	0,00429	-7,909
283	49,25	0,174028	0,00353	-1,749
288	89,13	0,309479	0,00347	-1,173
293	150,7	0,514334	0,00341	-0,665
298	147,9	0,496309	0,00336	-0,701
299	245,5	0,82107	0,00334	-0,197
300	260,3	0,867667	0,00333	-0,142
301	269,3	0,894684	0,00332	-0,111
302	285,4	0,945033	0,00331	-0,057
303	288,2	0,951155	0,00330	-0,050
304	300,3	0,987829	0,00329	-0,012
305	337,9	1,107869	0,00328	0,102
308	449,1	1,458117	0,00325	0,377
313	986,9	3,153035	0,00319	1,148
318	2301	7,235849	0,00314	1,979
323	2600	8,049536	0,00310	2,086
328	3460	10,54878	0,00305	2,356

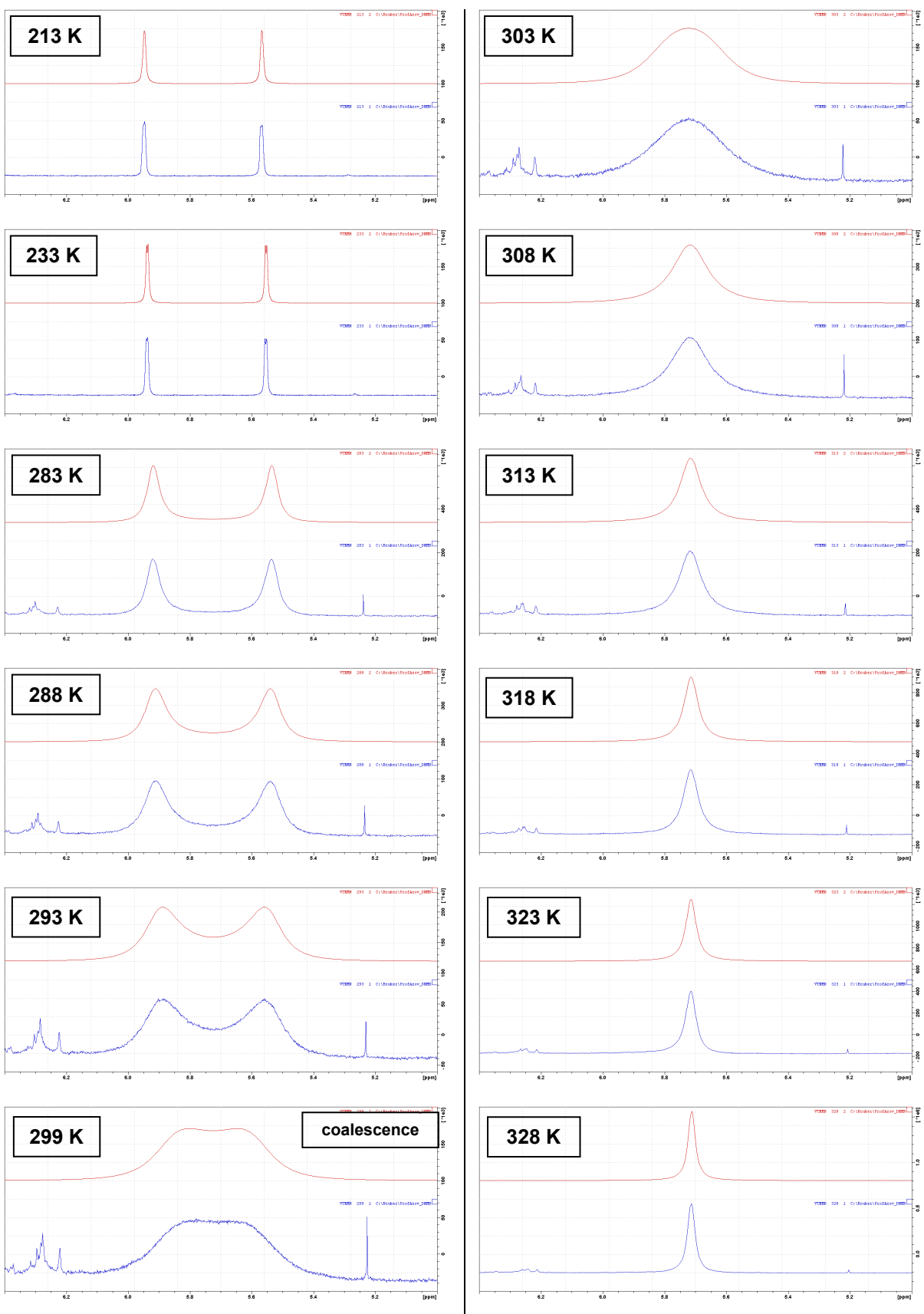


**Figure S5.** Fitting of the  $^1\text{H}$  NMR spectrum of **2** using  $\text{H}^{\text{H}}$  resonances measured at different temperatures (600 MHz,  $\text{CDCl}_3$ ). In each of the images the blue line below represents the measured spectrum, and the red line above represents the modelled spectrum.

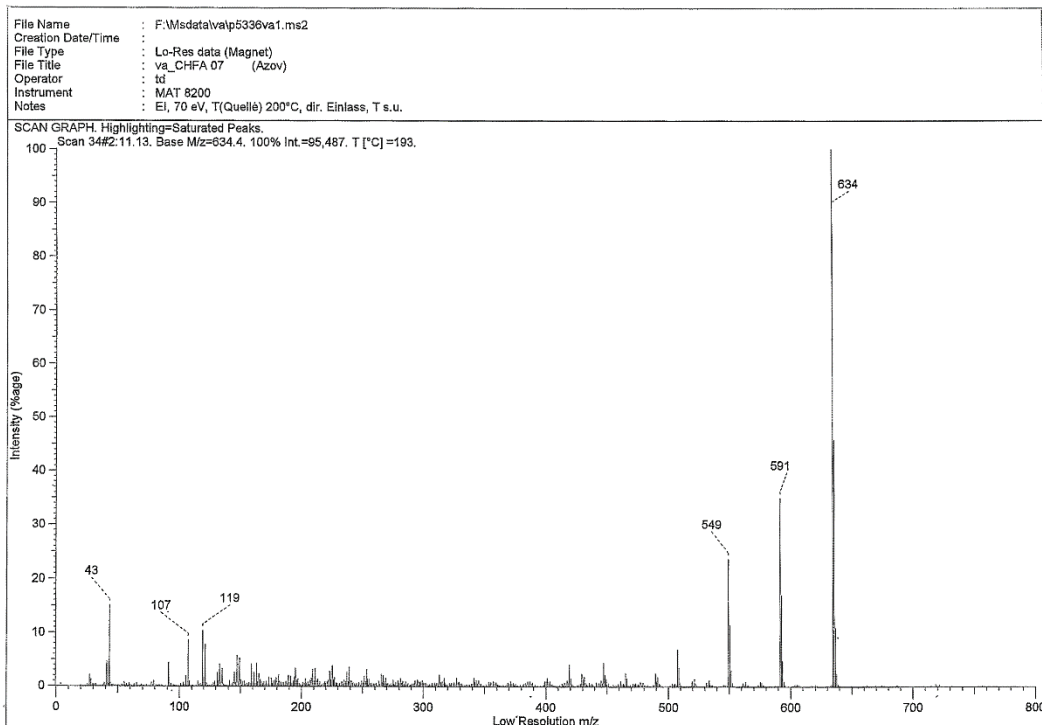


**Figure S6.** EI-MS (70 eV) spectrum of compound **3**. Signals at 591 and 549 u correspond to the loss of one ( $C_3H_7$ ) and two ( $C_3H_7 + C_3H_6$ ) propyl substituents on the low rim, respectively.

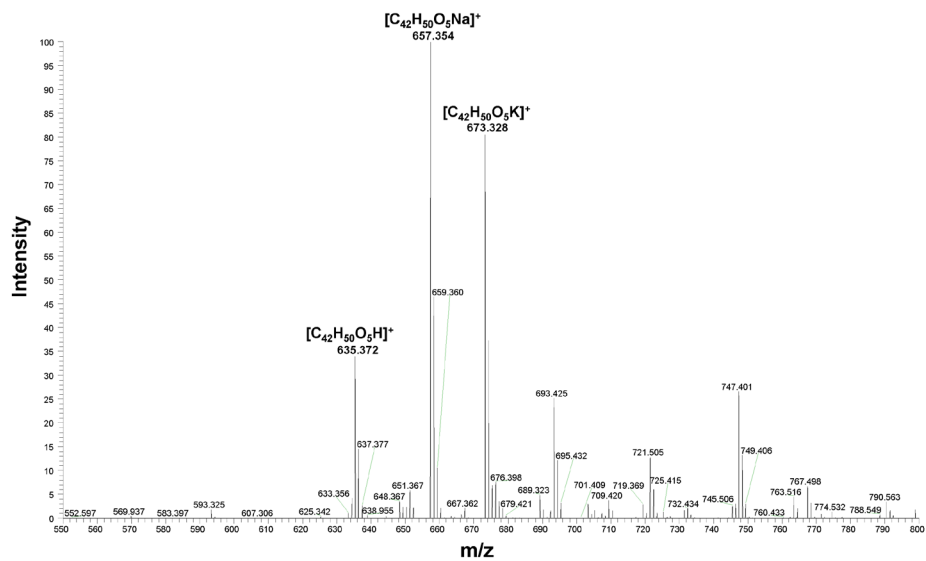


**Figure S7a.** ESI-MS (+) spectrum of compound **3**.

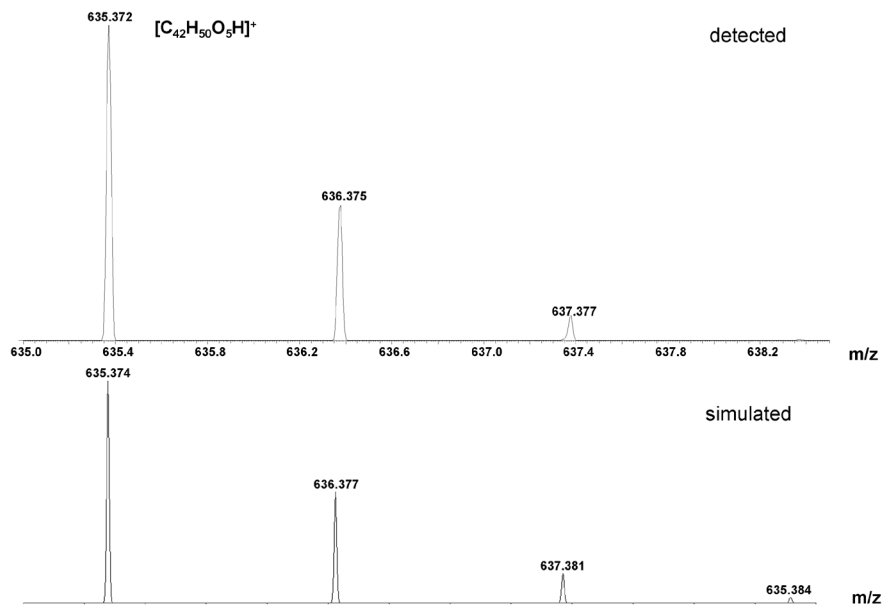


**Figure S7b.** ESI-MS and modelled pattern of the  $[C_{42}H_{50}O_5 + H]^+$  ion, generated upon ionization of compound 3.

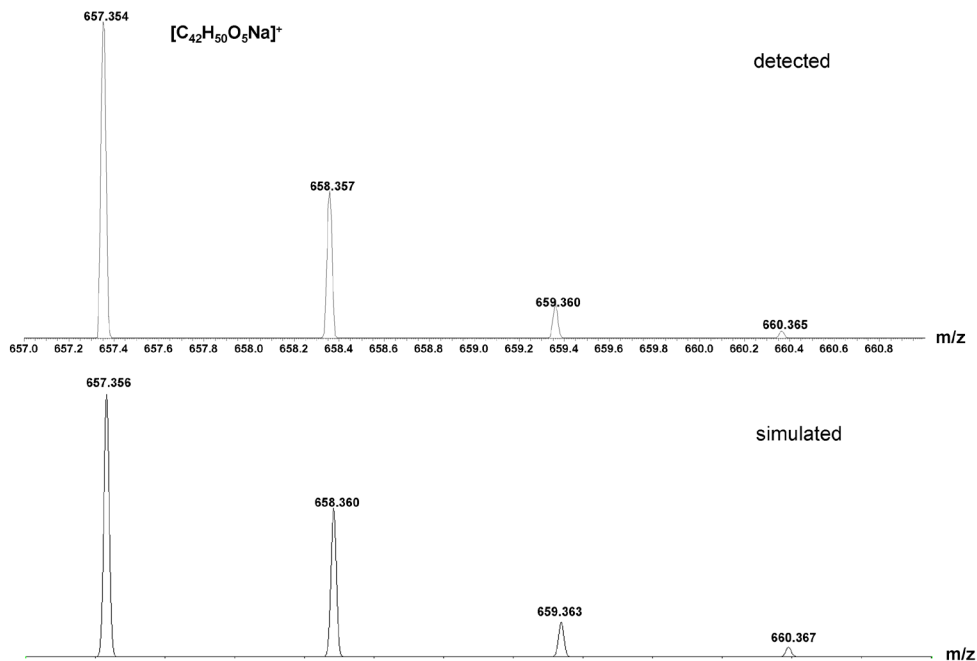


**Figure S7c.** ESI-MS and modelled pattern of the  $[C_{42}H_{50}O_5 + Na]^+$  ion, generated upon ionization of compound 3.

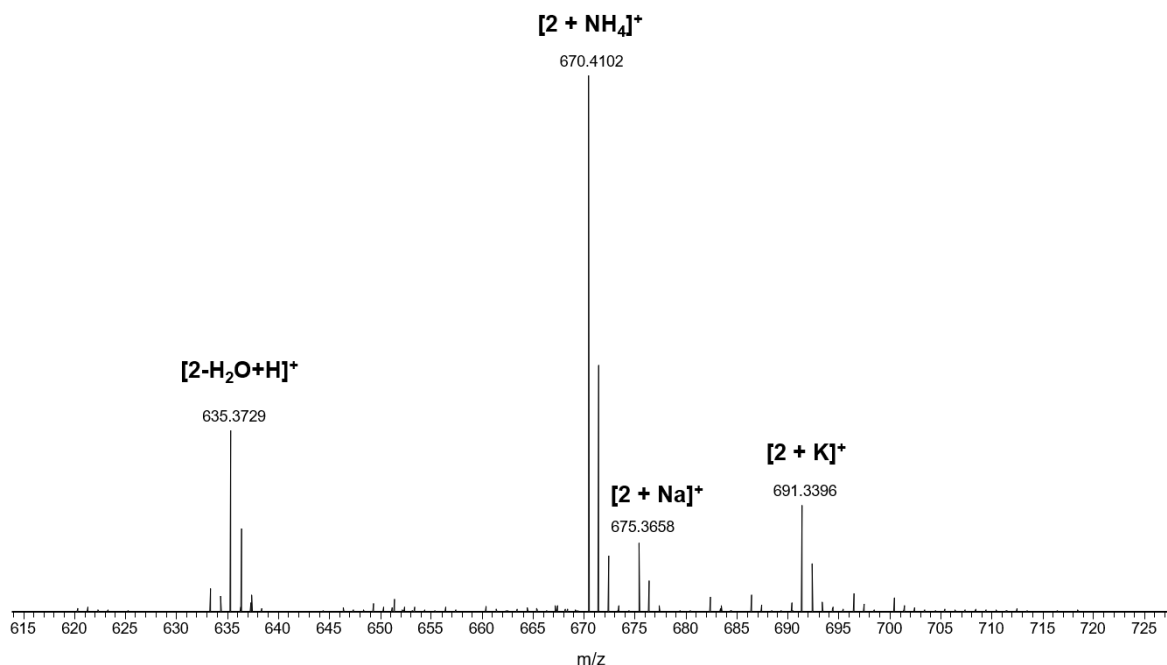


**Figure S8.** ESI-MS (+) spectrum of compound **2**.

Upon ionization, compound **2** did not show the expected  $[2+\text{H}]^+$  ion at  $m/z$  653, but only  $[2-\text{H}_2\text{O}+\text{H}]^+$  at  $m/z$  635 implying fast elimination of a water molecule with the formation of protonated  $[3+\text{H}]^+$  at  $m/z$  635. The alkali ion adducts  $[3+\text{Na}]^+$  and  $[3+\text{K}]^+$  and an ammonium ion adduct were found to be stable in the gas phase.

#### MS fragmentation experiments

Fragmentation study of compounds **2** and **3** was performed using a *Bruker Esquire3000 Plus* mass spectrometer. Fragment ions generated using in-source fragmentation were isolated in an ion trap and cooled by collisions with helium buffer gas. An adjustable alternating current voltage was then applied to initiate fragmentation reactions due to energetic collisions with He atoms.

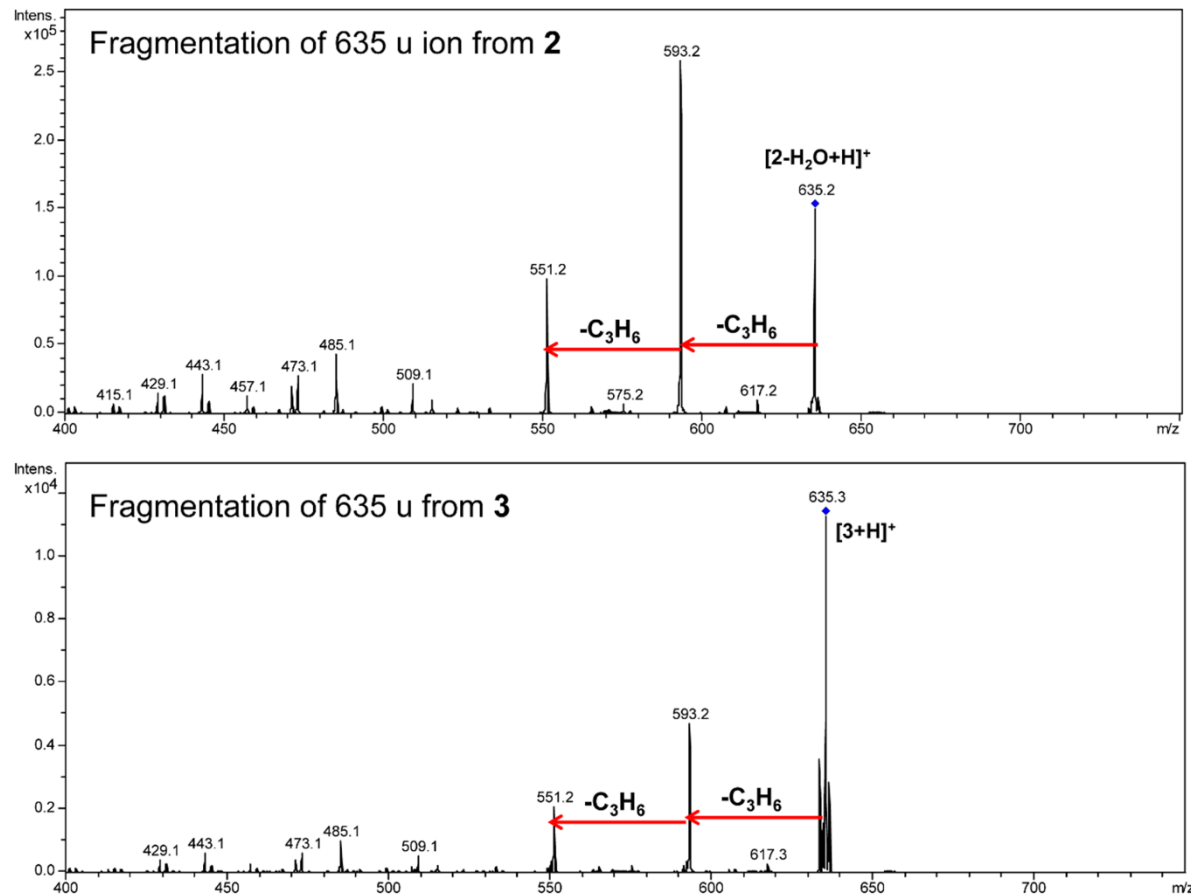


**Figure S9.** Fragmentation spectra of 635 u ion isolated after ESI(+) ionization of compounds **2** and **3**.

Isolation and fragmentation of ions at m/z 635 formed by ESI(+) of compound **2** and **3** demonstrate almost identical patterns.

## Computational details

The calculations of geometry optimization, transition state search, and vibration analysis were performed at the B3LYP/6-31g(d,p) level of theory using the *Gaussian 16* software.<sup>[1]</sup> The transition state (TS) search was performed both using the transition state optimization routine on an initial “guess” geometry with the symmetric central position of the ether bridge and using the *Synchronous Transit-Guided Quasi-Newton* (STQN) method<sup>[2]</sup> with the QST2 option. Both methods yielded the same TS structures, whose identity was confirmed by frequency calculations.

To account for dispersion and solvation effects, both the ground state geometry and the TS were re-optimized using the D3 dispersion correction with Becke-Johnson Damping<sup>[3,4]</sup> (GD3-BJ) and then both dispersion correction and solvation using the Polarizable Continuum Model<sup>[5]</sup> (PCM) for chloroform. The addition of the dispersion correction induced a noticeable influence on the energy of the transition state, lowering the barrier, whereas the PCM correction did not have much influence (Table S3). Changes in the molecular geometries of the ground and transition states after inclusion of dispersion correction and of solvation model were minimal.

**Table S3.** Energies of the lowest energy conformation and transition state for the conformational interconversion of two degenerate lowest energy conformations of **3** (R = Me) calculated at the B3LYP/6-31g(d,p) level of theory; without and with G3 dispersion correction (GD3-BJ) and PCM solvation in CHCl<sub>3</sub> (SCRF).

Structure	E, Hartree	E, kJ/mol	TS state, kJ/mol
Min	-1692.192551	-4442851.541	
Min, GD3BJ	-1692.392199	-4443375.72	
Min, GD3BJ + SCRF	-1692.399802	-4443395.679	
TS	-1692.16842	-4442788.187	63.35
TS, GD3BJ	-1692.371233	-4443320.673	55.05
TS, GD3BJ + SCRF	-1692.37859	-4443339.989	55.69

**Optimized Molecular Geometries of 3 (B3LYP/6-31g(d,p) + GD3-BJ + PCM in CHCl<sub>3</sub>)**

**Conf. 1**

O	-0.314000	2.996000	-1.811000
O	0.214000	-3.058000	-1.750000
O	1.648000	-0.034000	-1.589000
O	-1.746000	-0.008000	-1.532000
O	0.780000	0.080000	3.815000
C	1.877000	-0.217000	-2.984000
C	-2.036000	0.144000	-2.920000
C	-0.322000	4.406000	-2.016000
C	0.225000	-4.474000	-1.910000
C	2.805000	0.095000	-0.847000
C	-2.868000	-0.120000	-0.738000
C	2.316000	2.562000	-0.719000
C	-2.376000	-2.586000	-0.577000
C	2.727000	-2.402000	-0.494000
C	3.236000	1.379000	-0.482000
C	-0.231000	2.620000	-0.476000
C	-2.781000	2.387000	-0.444000
C	0.177000	-2.641000	-0.424000
C	3.441000	-1.065000	-0.376000
C	-3.284000	-1.395000	-0.328000
C	-3.484000	1.051000	-0.264000
C	1.035000	2.426000	0.107000
C	-1.065000	-2.436000	0.196000
C	4.437000	1.491000	0.229000
C	-1.412000	2.361000	0.235000
C	1.385000	-2.350000	0.236000
C	4.638000	-0.915000	0.332000
C	-4.453000	-1.491000	0.436000
C	-4.650000	0.917000	0.498000
C	5.155000	0.354000	0.601000
C	-5.154000	-0.345000	0.816000
C	1.093000	2.008000	1.438000
C	-1.073000	-1.971000	1.517000
C	1.326000	-1.887000	1.551000
C	-1.304000	1.943000	1.567000
C	-0.066000	1.761000	2.181000
C	0.107000	-1.690000	2.205000
C	0.032000	1.280000	3.616000
C	0.078000	-1.150000	3.622000
H	2.234000	0.708000	-3.455000
H	0.922000	-0.509000	-3.421000
H	-1.101000	0.423000	-3.405000
H	-2.416000	-0.791000	-3.353000
H	2.611000	-1.011000	-3.173000
H	-2.776000	0.935000	-3.095000
H	-0.389000	4.569000	-3.094000
H	0.253000	-4.670000	-2.985000
H	2.035000	2.639000	-1.772000
H	-2.136000	-2.686000	-1.638000
H	0.596000	4.875000	-1.637000
H	2.547000	-2.672000	-1.537000
H	-1.183000	4.880000	-1.525000
H	-2.641000	2.629000	-1.500000
H	-0.674000	-4.937000	-1.483000
H	1.107000	-4.927000	-1.438000
H	2.846000	3.485000	-0.456000
H	-2.899000	-3.503000	-0.275000
H	3.366000	-3.182000	-0.064000
H	-3.408000	3.176000	-0.012000
H	4.797000	2.477000	0.510000

H	5.154000	-1.800000	0.698000
H	-4.802000	-2.471000	0.752000
H	-5.150000	1.810000	0.865000
H	6.089000	0.455000	1.146000
H	-6.065000	-0.435000	1.401000
H	2.060000	1.816000	1.892000
H	-2.028000	-1.775000	1.997000
H	2.247000	-1.615000	2.059000
H	-2.212000	1.706000	2.116000
H	-0.964000	-1.050000	3.961000
H	-0.979000	1.168000	4.037000
H	0.557000	2.029000	4.221000
H	0.575000	-1.857000	4.296000

### Conf. 2

O	0.391000	-2.907000	-1.859000
O	-0.277000	3.016000	-1.724000
O	-1.638000	0.069000	-1.583000
O	1.678000	0.010000	-1.436000
O	-0.783000	-0.137000	3.827000
C	-1.862000	0.366000	-2.961000
C	1.874000	-0.162000	-2.838000
C	0.390000	-4.316000	-2.090000
C	-0.291000	4.436000	-1.873000
C	-2.791000	-0.102000	-0.849000
C	2.841000	0.148000	-0.712000
C	-2.248000	-2.545000	-0.799000
C	2.321000	2.597000	-0.581000
C	-2.764000	2.376000	-0.433000
C	-3.194000	-1.401000	-0.519000
C	0.286000	-2.566000	-0.518000
C	2.825000	-2.351000	-0.440000
C	-0.220000	2.598000	-0.403000
C	-3.450000	1.028000	-0.343000
C	3.255000	1.432000	-0.336000
C	3.501000	-1.005000	-0.264000
C	-0.988000	-2.396000	0.048000
C	1.028000	2.404000	0.202000
C	-4.373000	-1.562000	0.217000
C	1.452000	-2.324000	0.217000
C	-1.416000	2.301000	0.271000
C	-4.625000	0.835000	0.390000
C	4.438000	1.556000	0.399000
C	4.681000	-0.848000	0.470000
C	-5.105000	-0.452000	0.641000
C	5.165000	0.425000	0.774000
C	-1.070000	-1.994000	1.382000
C	1.060000	1.914000	1.512000
C	-1.339000	1.812000	1.574000
C	1.325000	-1.922000	1.550000
C	0.076000	-1.759000	2.146000
C	-0.110000	1.613000	2.207000
C	-0.044000	-1.336000	3.594000
C	-0.059000	1.076000	3.620000
H	-2.156000	-0.537000	-3.513000
H	-0.924000	0.757000	-3.353000
H	0.929000	-0.522000	-3.240000
H	2.153000	0.786000	-3.315000
H	-2.642000	1.124000	-3.087000
H	2.654000	-0.904000	-3.045000
H	0.475000	-4.458000	-3.170000
H	-0.336000	4.641000	-2.944000
H	-1.952000	-2.566000	-1.850000

H	2.069000	2.687000	-1.640000
H	-0.539000	-4.778000	-1.735000
H	-2.604000	2.683000	-1.468000
H	1.239000	-4.799000	-1.591000
H	2.704000	-2.606000	-1.495000
H	0.616000	4.889000	-1.454000
H	-1.166000	4.877000	-1.380000
H	-2.748000	-3.496000	-0.580000
H	2.818000	3.528000	-0.284000
H	-3.400000	3.133000	0.037000
H	3.452000	-3.126000	0.013000
H	-4.701000	-2.564000	0.479000
H	-5.148000	1.699000	0.791000
H	4.776000	2.545000	0.698000
H	5.206000	-1.731000	0.825000
H	-6.019000	-0.589000	1.209000
H	6.085000	0.534000	1.341000
H	-2.046000	-1.817000	1.823000
H	2.022000	1.717000	1.976000
H	-2.252000	1.526000	2.088000
H	2.223000	-1.693000	2.117000
H	0.987000	0.950000	3.933000
H	0.960000	-1.248000	4.035000
H	-0.586000	-2.104000	4.157000
H	-0.523000	1.798000	4.304000

### TS

O	-0.352000	3.049000	-1.687000
O	0.352000	-3.049000	-1.687000
O	1.613000	-0.265000	-1.513000
O	-1.613000	0.265000	-1.513000
O	-0.000000	-0.000000	4.180000
C	1.806000	-0.590000	-2.888000
C	-1.806000	0.591000	-2.888000
C	-0.173000	4.457000	-1.832000
C	0.173000	-4.457000	-1.833000
C	2.791000	-0.087000	-0.821000
C	-2.791000	0.087000	-0.821000
C	2.366000	2.371000	-0.990000
C	-2.366000	-2.371000	-0.990000
C	2.629000	-2.499000	-0.074000
C	3.296000	1.215000	-0.686000
C	-0.117000	2.588000	-0.401000
C	-2.629000	2.499000	-0.074000
C	0.117000	-2.588000	-0.401000
C	3.368000	-1.176000	-0.154000
C	-3.296000	-1.215000	-0.686000
C	-3.368000	1.176000	-0.154000
C	1.195000	2.303000	-0.010000
C	-1.195000	-2.303000	-0.010000
C	4.510000	1.390000	-0.018000
C	-1.208000	2.324000	0.444000
C	1.208000	-2.324000	0.444000
C	4.575000	-0.964000	0.523000
C	-4.510000	-1.390000	-0.018000
C	-4.575000	0.964000	0.524000
C	5.168000	0.299000	0.555000
C	-5.168000	-0.299000	0.555000
C	1.391000	1.793000	1.273000
C	-1.391000	-1.793000	1.272000
C	0.965000	-1.803000	1.721000
C	-0.965000	1.803000	1.722000
C	0.339000	1.533000	2.149000

C	-0.339000	-1.533000	2.149000
C	0.746000	1.013000	3.513000
C	-0.746000	-1.013000	3.513000
H	2.236000	0.258000	-3.437000
H	0.824000	-0.836000	-3.288000
H	-0.824000	0.837000	-3.288000
H	-2.236000	-0.258000	-3.437000
H	2.463000	-1.459000	-3.004000
H	-2.463000	1.460000	-3.004000
H	-0.373000	4.694000	-2.879000
H	0.373000	-4.694000	-2.880000
H	1.965000	2.327000	-2.005000
H	-1.965000	-2.327000	-2.005000
H	0.851000	4.760000	-1.581000
H	2.583000	-2.975000	-1.056000
H	-0.871000	5.012000	-1.193000
H	-2.583000	2.976000	-1.056000
H	-0.851000	-4.760000	-1.582000
H	0.871000	-5.012000	-1.194000
H	2.911000	3.318000	-0.895000
H	-2.911000	-3.318000	-0.895000
H	3.190000	-3.169000	0.586000
H	-3.190000	3.169000	0.586000
H	4.913000	2.393000	0.097000
H	5.042000	-1.796000	1.044000
H	-4.913000	-2.393000	0.097000
H	-5.042000	1.795000	1.044000
H	6.109000	0.444000	1.075000
H	-6.109000	-0.444000	1.075000
H	2.397000	1.532000	1.580000
H	-2.397000	-1.532000	1.580000
H	1.810000	-1.574000	2.364000
H	-1.810000	1.574000	2.365000
H	-1.790000	-0.681000	3.427000
H	0.744000	1.847000	4.228000
H	1.790000	0.681000	3.427000
H	-0.744000	-1.847000	4.228000

## References

- [1] M. J. Frisch, G. W. Trucks, H. B. Schlegel, G. E. Scuseria, M. a. Robb, J. R. Cheeseman, G. Scalmani, V. Barone, G. a. Petersson, H. Nakatsuji, X. Li, M. Caricato, a. V. Marenich, J. Bloino, B. G. Janesko, R. Gomperts, B. Mennucci, H. P. Hratchian, J. V. Ortiz, a. F. Izmaylov, J. L. Sonnenberg, Williams, F. Ding, F. Lipparini, F. Egidi, J. Goings, B. Peng, A. Petrone, T. Henderson, D. Ranasinghe, V. G. Zakrzewski, J. Gao, N. Rega, G. Zheng, W. Liang, M. Hada, M. Ehara, K. Toyota, R. Fukuda, J. Hasegawa, M. Ishida, T. Nakajima, Y. Honda, O. Kitao, H. Nakai, T. Vreven, K. Throssell, J. a. Montgomery Jr., J. E. Peralta, F. Ogliaro, M. J. Bearpark, J. J. Heyd, E. N. Brothers, K. N. Kudin, V. N. Staroverov, T. a. Keith, R. Kobayashi, J. Normand, K. Raghavachari, a. P. Rendell, J. C. Burant, S. S. Iyengar, J. Tomasi, M. Cossi, J. M. Millam, M. Klene, C. Adamo, R. Cammi, J. W. Ochterski, R. L. Martin, K. Morokuma, O. Farkas, J. B. Foresman, D. J. Fox, **2016**, Gaussian 16, Revision C.01, Gaussian, Inc., Wallin.
- [2] C. Peng, P. Y. Ayala, H. B. Schlegel, M. J. Frisch, *J. Comput. Chem.* **1996**, 17, 49–56.
- [3] S. Grimme, J. Antony, S. Ehrlich, H. Krieg, *J. Chem. Phys.* **2010**, 132, 154104.
- [4] S. Grimme, S. Ehrlich, L. Goerigk, *J. Comput. Chem.* **2011**, 32, 1456–1465.
- [5] B. Mennucci, *WIREs Comput. Mol. Sci.* **2012**, 2, 386–404.